2020 IEEE/RSJ International Conference on Intelligent Robots and Systems (IROS)
October 25-29, 2020, Las Vegas, NV, USA (Virtual)

An In-Pipe Manipulator for Contamination-Less Rehabilitation of Water Distribution Pipes

Yip Fun Yeung[1] and Kamal Youcef-Toumi, *Senior Member, IEEE*[1]

***Abstract*— The recent development of in-pipe robots (IPR) with locomotion and inspection functions provides a new possibility to water distribution pipe maintenance - to rehabilitate pipe defects internally. Yet only a limited number of Rehabilitation in-pipe robots (R-IPR) have been proposed. One primary concern that impedes the development of Rehabilitation in-pipe robots is the excessive amount of contamination generated during the rehabilitation process. Correspondingly, we propose a novel concept: Contamination-Less in-pipe Rehabilitation (CLR) and develop the CLR in-pipe robot as an innovative solution.**

The proposed robot contains three modules for pipe-surface sealing, pipe-wall cleaning, and in-pipe manipulation. This paper centers on the comprehensive design of the manipulator module. First, the manipulator features a high-DoF configuration to deploy the other two modules simultaneously. Second, the configuration adopts a nested-outer-inner architecture to ensure the seal always encloses the pipe-wall cleaning device. The holistic and detailed design process of the manipulator, including design concept, kinematics, load requirements, design for manufacturing, and simulated deployment, are presented. Eventually, the fully implemented robot accomplished the first Contamination-Less in-pipe Rehabilitation.

Keywords: Service Robotics; Product Design, Development and Prototyping; Kinematics.

I. INTRODUCTION

Water pipeline maintenance is a severe and global issue. In the United States and Canada, more than 10% of the distributed water is lost on its way to the consumers, and over 240,000 water main breaks can happen annually [1]. In developing countries, water loss rates can be up to 40% [2][3]. Despite the urgency in saving water, the most widely applied method for water pipe rehabilitation is still replacing the entire pipe section after a water-main outburst takes place. Other preventative practices utilize heavy-duty machinery such as mechanical grinders, metal scrappers, and hydro-jets to remove pipe corrosion asperities [4], normally referred to as tubercle. This type of task, categorized as open-cut rehabilitation, is insensitive to potential outbursts, largely constrained by the pipe diameter, and requires a complete shut-off of water service.

Rehabilitation in-pipe robots (R-IPR) bring an alternative method to the industry, which is to conduct rehabilitation on the internal surface of pipes. Thinh et al. propose an R-IPR that is equipped with a cleaning disk, which has approximately the same diameter as the pipe. It removes tubercle while the robot moves along the pipeline [5]. The DeWaLop robot by Mateos et al. [6], and the PROKASRO robot [7] each use a multi-DoF in-pipe manipulator and an onboard grinder for the corrosion removal task. However, a vital problem is ignored by IPR researchers, which is the excessive amount of contamination generated during the rehabilitation process. The harmful byproduct, if not adequately contained, can significantly increase the virus content downstream of the pipe network [8] and lead to severe consumer health issues [9]. Unfortunately, to the author's knowledge, no existing R-IPR has taken into account the contamination concern.

Correspondingly, we propose, design and implement the **C**ontamination-**L**ess **R**ehabilitation (CLR) in-pipe robot to accomplish the following tasks:

1) Conduct general in-pipe rehabilitation.
2) Meanwhile, prevent by-produced debris from contaminating the pipeline.

While pipe rehabilitation typically requires multiple operations, namely, pipe-wall cleaning of tubercle, leak site repair, and post-treatment of anti-corrosion layer [10], in this work, the objective narrows down to deliver the pipe-wall cleaning task, since it is often the most intense operation in terms of byproduct generation.

The most critical on-board component is an in-pipe manipulator. Its objective is to deploy a specialized mechanical seal [11] to create a water-tight enclosure against corroded pipe surfaces and manipulate a cleaning device to remove tubercle within the enclosure so that no induced debris contaminates the pipeline. This requires the in-pipe manipulator to embody a high degree-of-freedom (DoF) layout, and sets of complex mechanism to decouple the manipulation of the seal and the cleaning device. On the other hand, the in-pipe environment is exceedingly constricted. Notably, in this work, the des-

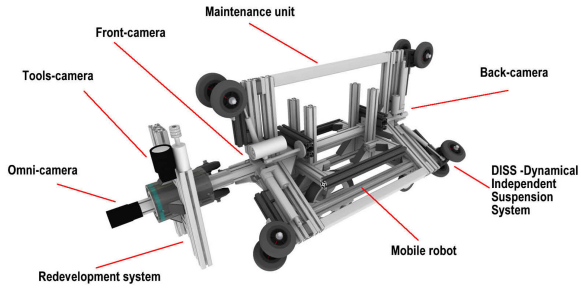

Fig. 1. In state-of-the-art R-IPR systems [6], no measure is taken to contain the contamination generated by the rehabilitation operation.

*This work was supported by MathEarth.Inc

[1]The authors are with the Mechatronics Research Laboratory in the Department of Mechanical Engineering, Massachusetts Institute of Technology, Cambridge, MA, 02139, USA. Email: {yyeung, youcef}@mit.edu

ignated deployment scenario is a $100mm$-diameter pipe, a very restrained workspace even compared within the IPR community. These two contrasting features make the design of the in-pipe manipulator challenging.

This paper centers on the comprehensive design process of the in-pipe manipulator. It features a novel nested-outer-inner layout. In Section II, we first introduce the comprehensive functional requirements (FR) of the CLR robot and its projection on the manipulator. We demonstrate the system-level design of the overall manipulator in Section III, including a review of common manipulator layout and design justifications, which we believe will be heuristic to the general R-IPR development community. The detailed development of individual components is covered in Section IV. In Section V, a manipulator prototype is implemented and integrated with the other components of the robot. Preliminary evaluations are carried out in Section VI, and finally, the robot conducted a proof-of-concept CLR rehabilitation for a real corroded pipe, the first deployment of its kind.

II. Functional Requirements

The Contamination-Less Rehabilitation in-pipe robot is a continuation of the IPR series from the MIT Mechatronics Research Laboratory (MRL). With the MRL locomotion robot (L-IPR) [12], it is presumed that in the cylindrical coordinate of a water distribution pipe, $O_{r,\theta,z}$, the CLR robot can be grounded at arbitrary positions along the pipeline, i.e., z-axis, and is always centered at the geometric center of the pipe's cross-section, i.e., $r = 0$. In addition, with the MRL inspection IPR (I-IPR) [13], the profiles of local tubercle asperities are assumed as prior knowledge. The integration of the L-IPR, I-IPR, and CLR robot is beyond the scope of this study.

The overall objective is to develop an in-pipe device to perform a pipe-cleaning task for corroded water distribution pipes while containing by-produced contamination. Three sub-tasks are involved: pipe surface cleaning, contamination containment, and end-effector manipulation. After rounds of careful screening, we determine to use an electric grinder, a mechanical seal, and an in-pipe manipulator to address the three sub-tasks, respectively. Further demonstrated in Fig.2-D, the seal physically encompasses the electric grinder at all times, and both end-effectors are installed on the manipulator. The rehabilitation routine schemes as follows:

1) The manipulator engages the seal by compression against the corroded pipe wall to form a water-tight enclosure around the cleaning device.
2) The manipulator operates the cleaning device, i.e., the electric grinder, to remove the tubercle asperities, while maintaining the water-tight enclosure.
3) An external fluid pump circulates rinsing water through the enclosure and collects contained debris.
4) The manipulator disengages the seal and repeats procedure 1) - 3) at the next corrosion site.

From this routine, detailed functional requirements and correlated design specifications for the manipulator are derived:

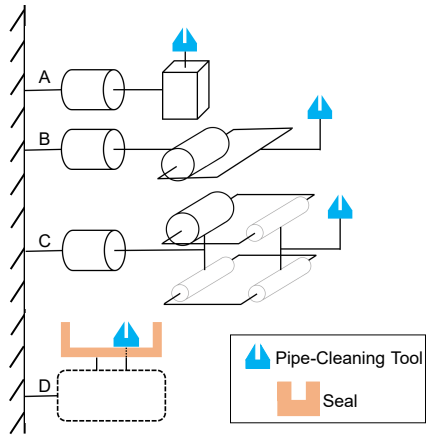

Fig. 2. A-C: Schematics of state-of-the-art R-IPR configurations. D: The proposed manipulator requires that the cleaning device is constantly encompassed by the seal.

1) Engage the seal to form an enclosure against the corroded pipe surface.
   a) This entails a configuration to satisfy the DoF requirement of the seal.
   b) This entails a sufficient load capacity to engage the seal by compression.
2) Deploy the cleaning device while the seal is engaged.
   a) This entails extra DoF of the cleaning device that is super-positioned on the seal's DoF.
   b) This entails a sufficient load capacity for the cleaning device to remove tubercle.
   c) This entails a nested configuration such that the workspace of the cleaning device is contained by the sealed enclosure.

Listed above are the fundamental functional requirements for the CLR robot. Other FRs include but are not limited to, the size constraint for an IPR to maneuver through pipe bents [14], and compatibility with other on-board components, in terms of physical size and functionality. In addition, the targeted deployment scenario is a $100mm$ diameter pipe. This is a critical requirement but is not especially emphasized because the proposed design methodology is expected to be scalable across a wide range of deployment scenarios.

III. System-Level Design

In this section, we demonstrate a step-by-step system-level design process of the CLR robot, from potential configuration candidates to the final kinematic layout. Since the Contamination-Less Rehabilitation concept is proposed for the first time, we believe that detailing the design and validation process is beneficial and heuristic to the general IPR community.

Unlike most industrial robots at factory plants, which are barely constrained by the environment, IPRs are specially regulated by the cylindrical geometry of a pipe. The series revolute-prismatic manipulator, demonstrated in Fig.2-A, gains popularity as it directly constructs a cylindrical

workspace. An example is the DeWaLop robot [6] shown in Fig.1. Similar to a SCARA robot, it takes advantage of the mechanical stiffness of each link to perform high payload operations. A slight variation replaces the prismatic joint with a revolute one, as depicted in Fig.2-B. It finds a balance between load capacity and mechanism complexity. The prevailing R-IPR configuration is demonstrated in Fig.2-C. It utilizes a closed-loop kinematics chain, more specifically, a set of parallelogram linkage is integrated on the second revolute joint to linearize the revolute motion, keeping the end-effector constantly normal to the pipe surface. Referred to as $RR-C$ in this study, this configuration is adopted by most commercial R-IPRs, including the PROKASRO robot [7] and the KA-TE robot [15]. The above configurations are suitable for tubercle-removal tasks, but no measure is taken to prevent a large amount of by-produced debris from contaminating the pipeline during the rehabilitation operation, making the deployment of such R-IPRs risky and impractical.

Other manipulator configurations that aim at retaining high DoF while minimizing sizes, such as micro tendon-driven manipulators [16] and spherical parallel manipulators [17], also inspire the generation of many design concepts, the representative ones are displayed in Fig.3.

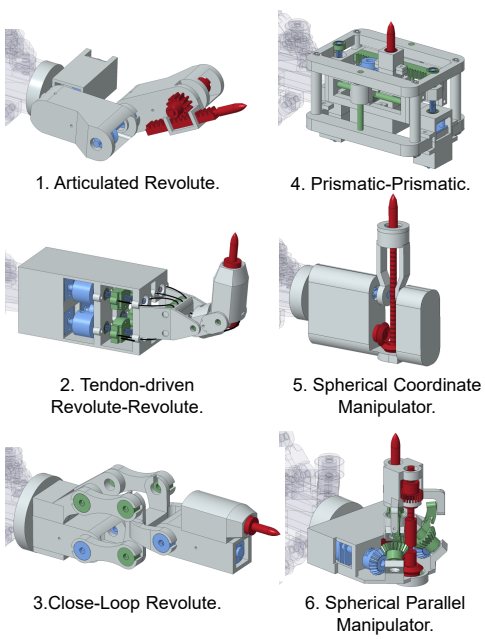

Fig. 3. Design concepts of the CLR robot. The first revolute joint about the z-axis is hidden because it is a fundamental component for all concepts.

One prototype for each concept is constructed for evaluation. Critical design metrics and corresponding scores are recorded in Table.I, with the articulated revolute concept as the baseline. The finalized manipulator configuration features a hybrid nested-outer-inner configuration, as illustrated in Fig.4. The outer manipulator employs a bi-articulated-$RR-C$ arrangement to manipulate the seal in the cylindrical coordinate, and the inner adopts a series prismatic-prismatic PP configuration for Cartesian-Coordinate manipulation.

TABLE I
CONCEPT SCORING FOR THE MANIPULATOR

Design Metrics	Imp.	1	2	3	4	5	6
Degree of Freedom	M-H	0	0	0	0	0	0
Compactness	M-H	0	-1	-1	1	1	-1
Actuator Count	M	0	-2	0	0	0	0
Payload	M	0	-1	0	1	0	2
Design for Manufacturing	M	0	-2	0	-1	-1	-2
Design for Assembly	M	0	-1	-1	-1	-1	-2
Cyl-Coord. Manipulation	H	0	0	1	0	2	2
Cart-Coord. Manipulation	M	0	0	1	2	-1	-1
Range of Motion	M	0	0	0	0	0	-2
Back-drivability	M	0	-2	0	2	-1	1
Material Availability	L-M	0	-1	0	0	0	-1
Displaced Inertia	L-M	0	3	1	0	0	1

The seal and the cleaning device are installed on the outer and inner manipulator, respectively, to ensure the seal is constantly encompassing the workspace of the cleaning device. The local coordinate frame at each joint is defined as O_i, where $i \in [1, 2, 2', 3, 4]$ are the joint and link numbers; the base frame is denoted as O_0. An intermediate coordinate frame, $O_{2'}$, is defined to describe the parallelogram linkage conveniently. The positions of the seal, measured at the geometric center of the base, and the cleaning device, measured at the tip of the tool bit, with respect to O_i are denoted as $\boldsymbol{p_{sl,i}}$ and $\boldsymbol{p_{cln,i}}$, respectively.

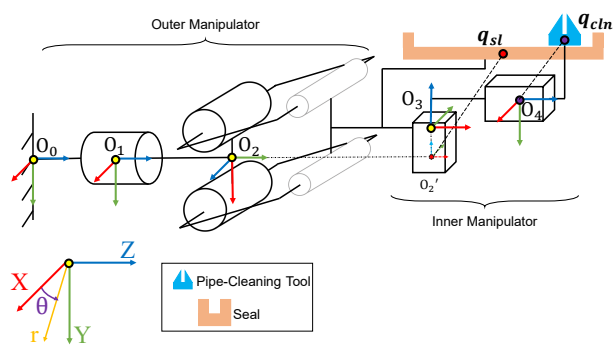

Fig. 4. Schematics of the proposed outer-inner CLR manipulator. The seal and the cleaning tool are mounted on the outer and inner manipulator, respectively. Global and local coordinate frames are defined as shown.

IV. DETAILED DESIGN

The global manipulator design is revealed in Fig.5. As depicted on the bottom left, the customized mechanical seal is installed directly on the outer manipulator in the fully integrated model. An electric grinder is installed on the inner manipulator as the pipe-cleaning tool. In this section, designs for the outer and inner manipulators are presented in detail.

A. Outer Manipulator

The outer manipulator consists of three links, $i = 0, 1, 2$, and two joint, $i = 1, 2$, as displayed by Fig.6-A. In practice,

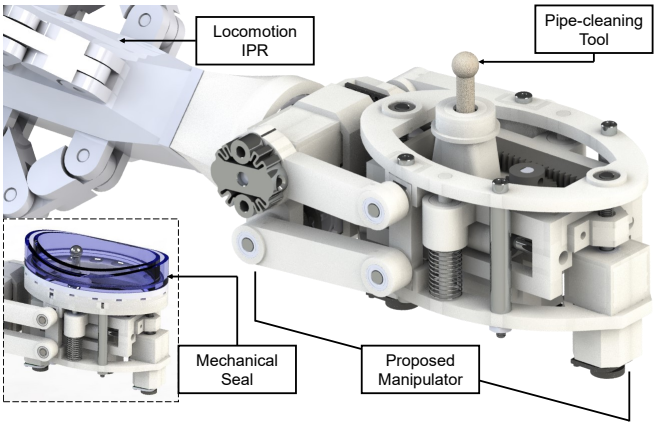

Fig. 5. Demonstration of the proposed R-IPR. It is presumed to be mounted on an L-IPR. Bottom Left: In the fully integrated model, the seal is installed directly on the outer manipulator to encompass the cleaning tool.

Link-0 is integrated as part of the L-IPR, on which the CLR is grounded. The outer manipulator is in charge of engaging the mechanical seal and coarse movement of the pipe-cleaning tool. Thus, it bears large moment loads when both end-effectors are in action. Since the loading direction is normal to Joint-1, the mechanical stiffness at Link0-Joint1-Link1 is specially reinforced with a high-radial-load ball bearing. For Joint-2, the moment load is fully supported by the actuator. As a result, a pair of actuators are utilized, forming a bi-articulated joint to double the load capacity. In addition, a closed-loop-parallelogram-linkage Link-2 allows a nearly prismatic motion along the radial direction r. Link-2

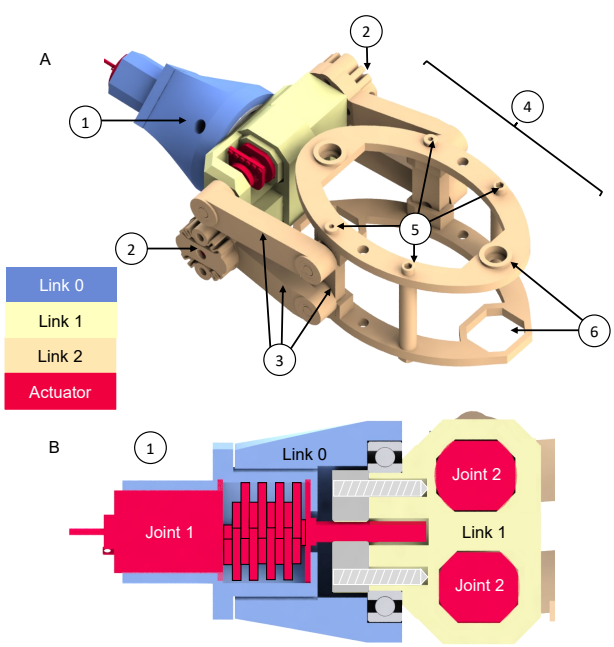

Fig. 6. A: Components of the outer manipulator. -1: Link0-Joint1-Link1. -2: Torsional spring for the serial elastic joint. -3: Parallelogram linkage. -4: Enclosure frame of the inner manipulator. -5: Installation ports for the seal. -6: Installation ports for the inner manipulator. B: Cross-sectional view of Link0-Joint1-Link1.

also embodies the enclosure frame, within which the inner manipulator operates. Mounting interfaces for the seal and the inner manipulator are integrated into the frame of Link-2 at A-5 and A-6, respectively.

As the seal is mounted rigidly on Link-2, its position, $\boldsymbol{p_{sl,i}}$, can be expressed with the Denavit–Hartenberg (D-H) parameters listed in Table, II, where the displacement of Joint-i is denoted as q_i. The position of the seal with respect to coordinate frame $O_{2'}$ is given as:

$$\boldsymbol{p_{sl,2'}} = [5, 0, 20]^T [mm] \tag{1}$$

The rehabilitation operation involves a high degree of interaction between two rigid bodies, i.e., the robot and the pipe wall, which can pose potential hazards to the robot's hardware. A passive yet effective solution is to use a Serial Elastic Actuator (SEA) is a passive and efficient way to address this problem [18]. As demonstrated in Fig.6-A-2, a torsional spring is used as the coupling between Joint-2 and Link-2. In principle, it serves as a mechanical low pass filter that attenuates high-frequency vibration induced from the pipe-cleaning operation. The installation is modular, more precisely, the spring can be replaced for upgrade or maintenance without disassembling any other component. Since high-speed manipulation is not a critical requirement for the rehabilitation operation, the fact that SEA lowers the system bandwidth is not a particular concern.

TABLE II

DENAVIT–HARTENBERG PARAMETERS FOR THE SEAL

i	$\boldsymbol{a_i}[mm]$	$\boldsymbol{d_i}[mm]$	$\boldsymbol{\alpha_i}[rad]$	$\boldsymbol{\theta_i}[rad]$
0	0	0	0	0
1	0	10	0	0
2	0	22	$-\frac{\pi}{2}$	q_1
2'	$14+35\times\cos(q_2)$	0	$-\frac{\pi}{2}$	$\frac{\pi}{2}$

B. Inner Manipulator

The inner Cartesian-Coordinate manipulator is in charge of the fine movement of the grinding device while the seal is engaged by the outer manipulator. The electric grinder is installed on Link-4, as demonstrated in Fig.7. The manipulation routine after the seal is in place is proposed as follows:

1) While the seal is engaged by the outer manipulator:
   a) Turn on the electric grinder.
   b) Extraction and retraction of the electric grinder along the r-direction to remove tubercle.
   c) Turn off the electric grinder.
   d) Manipulate the electric grinder along the z-direction to reach the next asperity.
   e) Repeat a)-c) until all tubercle asperities in the workspace are cleared.
2) Outer manipulator manipulates both end-effectors to the next angular position, θ and radial position, r.
3) Repeat 1) and 2) until breakpoint.

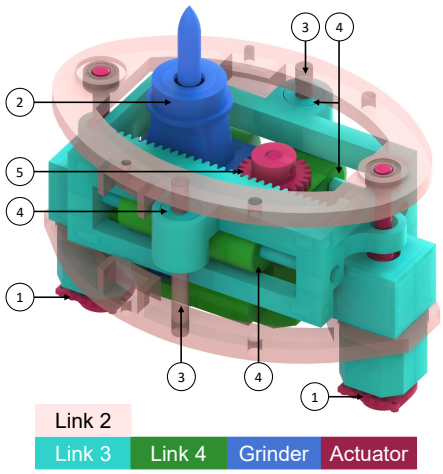

Fig. 7. Components of the inner manipulator. -1: Lead-screw transmission on Joint 3. -2: The electric grinder. -3: Linear slides. -4: Linear bearings. -5: Rack and pinion transmission on Joint 4

The extraction and retraction operation requires a high linear payload to thrust the grinder into the asperities. Thus, Joint-3 utilizes a pair of lead-screw type transmission, indicated by Fig.7-1. Joint-4 practices routine 1-d. Since the grinder is not in contact with any tubercle asperity at this step, the load requirement for Joint-4 is not considerable. Consequently, a rack-and-pinion transmission is adopted for its quick response and trivial complexity, as shown in Fig.7-5. Additionally, two pairs of sliding rails and linear bearings are employed for each of Joint 3 and 4 to avoid incidental deformation during operation. The DH parameters for $i = 3, 4$ are defined in Table.III. The position of the cleaning device with respect to coordinate frame O_4 is:

$$\boldsymbol{p_{cln,4}} = [0, -17 + q_4, L_{bit}]^T [mm] \tag{2}$$

where L_{bit} is the length of the grinding bit.

It is worth emphasizing that the tubercle-removal routine is meticulously planned as multiple orthogonal grindings along the z-axis. An alternative routine is to conduct face-grinding along the z-axis without retracting the cleaning bit. To accomplish this alternative, a high-payload transmission and a high-precision gantry system are needed for Joint 4.

TABLE III

DENAVIT–HARTENBERG PARAMETERS FOR THE CLEANING DEVICE

i	$\boldsymbol{a_i}[mm]$	$\boldsymbol{d_i}[mm]$	$\boldsymbol{\alpha_i}[rad]$	$\boldsymbol{\theta_i}[rad]$
3	0	$35\times\sin(q_2)$	0	$-\frac{\pi}{2}$
4	0	q_3	$-\frac{\pi}{2}$	$\frac{\pi}{2}$

V. HARDWARE FABRICATION AND INTEGRATION

In this section, we implement the finalized CLR robot design. Particularly, we present the process of material selection, component fabrication, and system integration in detail.

In a concurrent work, we propose a compound mechanical seal for the CLR robot. It features a multi-layer compound structure to deal with two characteristics of tuberculated pipe surfaces: 1. macroscopical surface roughness, 2. overhang in foundation profile. The mechanical seal requires a 45% lower compression load than off-the-shelf seals to function [11]. Specifically, the mechanical seal requires less than $90N/m$ unit force to create a water-tight enclosure on mildly corroded pipe surfaces with tubercle asperities up to 4mm tall. The circumference along the center-line of the seal is $212mm$.

For the tubercle removal task, a 2300RPM-1.1W-DC motor is used to power a $3mm$-diameter grinding bits. Unfortunately, no reference is found on the load requirement to demolish a piece of tubercle asperity. Consequently, a bench-top experiment is conducted to determine the practical load requirement, as displayed in Fig.8. The grinder setup is attached to a press bench, which thrust the grinder into a piece of corroded sample. It is recorded that a maximum pressing force of $8N$ is sufficient to completely remove $4mm$ tall tubercle asperity in the worst case, i.e., from a heavily corroded pipe surface.

Fig. 8. Demonstration of the bench-top experiment. Right: On mildly corroded surfaces, tubercle asperities break off effortlessly with neighboring asperities. Left: On heavily corroded surfaces, neighboring tubercle asperities do not easily break off, even with a larger thrust force.

Based on the loading requirements, actuation methods for each joint are detailed in Table.IV. A fully integrated CLR robot is constructed and depicted in Fig.9-A, including the manipulator module, the sealing module, and the pipe-cleaning grinder. Fused Deposition Modelling is used to

TABLE IV

DETAILS OF ACTUATION

Joint	Actuation	Qty.	Transmission	Stall Load
1	Pololu Micro Metal Gearmotor HPCB 6V	1	1000:1 Gearbox	$11.0kgcm$
2	Pololu Micro Metal Gearmotor HPCB 6V	2	1000:1 Gearbox	$22.1kgcm$
3	DC 6V Gear Motor	2	150:1 Gearbox and M3-$55mm$ lead screw	$4.8kgcm$ ($15.8N$)
4	Pololu Micro Metal Gearmotor HPCB 6V	1	150:1 Gearbox and Module 0.5 rack-and-pinion	$2.0kgcm$

fabricate low load-bearing and bulky components. For high-resolution components, Digital Light Processing printers are used. The SEA is fabricated with wired Electrical Discharge Machining. Its stiffness is computed with Finite Element Analysis in ANSYS, indicating $k_{SEA} = 135[Nm/rad]$. In terms of integration, an exploded view of the CLR robot in Fig.10 demonstrates its modularity. The grinding bit and the grinding motor are connected via a flexible coupling in Fig.9-B, such that the bit can be easily replaced for other operations. In Fig.9-C, a mobile interface on the seal is connected with the grinder, to ensure no liquid leaks into the inner manipulator during the rehabilitation operation.

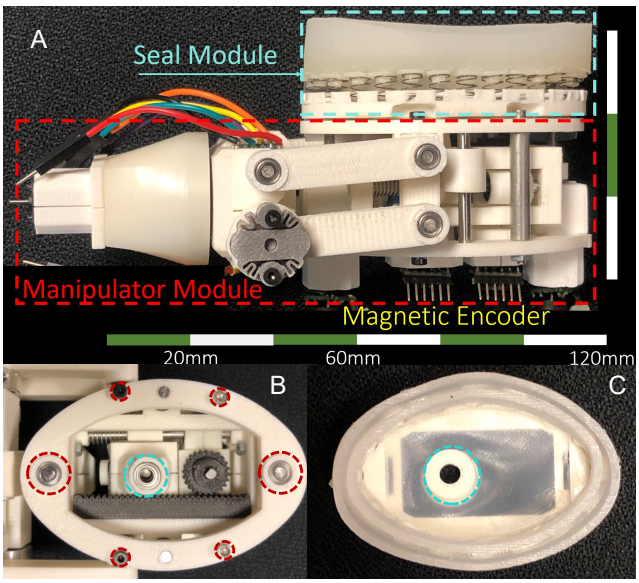

Fig. 9. A: Demonstration of the integrated CLR robot. B. Red: Installation ports of the seal; Blue: Flexible coupling between grinder and grinding bit. C. Mobile interface.

Position-PID controllers and a velocity-PID controller are implemented for the joints and the grinder, respectively. An incremental magnetic encoder is installed on each actuator for feedback. The controller parameters are tuned via the Ziegler Nichols method. At the ongoing development stage, the manipulator is controlled manually by an operator with multiple analog inputs. The limitation of controlling only the position is discussed in Sec.VII.

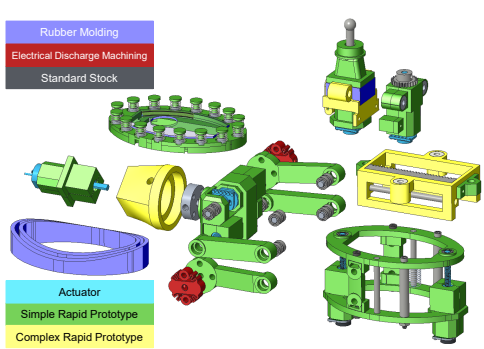

Fig. 10. An exploded view of the CLR robot assembly.

VI. Preliminary Evaluation and Deployment

In this section, preliminary evaluations of the CLR manipulator are conducted via virtual simulations and a dry run in a $100mm$-diameter PVC pipe. Finally, for the first time, a Contamination-Less Rehabilitation in a real corroded pipe is conducted.

A. Simulated Environment

Throughout the development process, the iterative designs are constantly tested in Simscape Multibody to achieve the optimal balance between the kinematics and the manipulator's physical size. The workspace of the finalized design is illustrated in Fig.11. For an operation to clean an approximately $10mm$ by $15mm$ area on the pipe surface, the desired trajectory of each joint is presented on the left. The corresponding trajectory of the electric grinder in the position space is displayed on the right portion. The grinding bit successfully reaches the pipe surface when the manipulator is grounded at the geometric center of the pipe's cross-section, i.e., $r = 0$. In addition, the bit can be retracted by a maximum distance of $8.7mm$, to minimize the volume of the CLR robot. The retraction distance is greater than the targeted asperity height, $4mm$, as a redundant measure in case of excessively big tubercle.

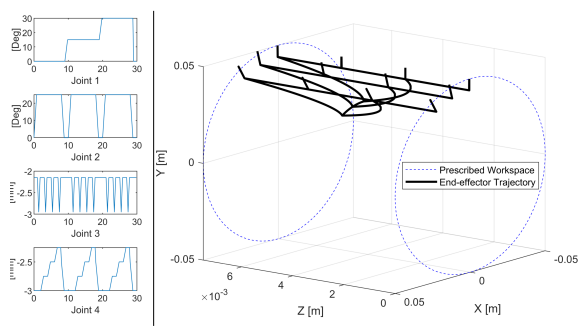

Fig. 11. The trajectory of the end-effector in Simscape Multibody's virtual environment. The manipulator kinematics are iteratively evaluated and updated.

To evaluate the real kinematics and actuator responses, the implemented CLR robot prototype is deployed in a $100mm$-diameter PVC pipe section. Mock tubercle pieces are fabricated with Fused Deposition Modelling and attached to the pipe wall to simulate a corroded pipe environment. In Fig.12 A-E, the grinding bit is manipulated with manual operation. It is illustrated that the implemented manipulator indeed execute the proposed kinematics. Additionally, the operator can create small holes by grinding with a tungsten carbide bit on the mock tubercle in Fig.12-F. Given that the 3D-printed parts are orders of magnitude harder than real tubercle asperities, the deployment concludes that the manipulator satisfies the load and kinematic requirements. Particularly, the maximum current provided by the dual actuators in Joint-2 is $2.2A$, corresponding to approximately $16.8kgcm$ of delivered torque, approximately twice the maximum load required to deploy both end-effectors.

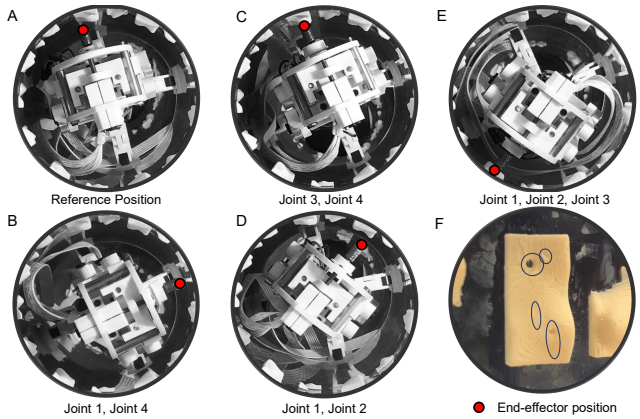

Fig. 12. Demonstration of the in-pipe manipulation. Mock tubercle asperities are attached to a $100mm$-diameter PVC pipe. A-E: End-effector at various locations relative to the pipe wall by actuating the corresponding joints. F: Small holes are created by grinding with a tungsten carbide bit. Note that the bit skids on the surface, as shown in the circles. Improving hardware precision is a way to mitigate this issue.

Although the control system is not the focus of this study, a preliminary actuator response evaluation is conducted to ensure the coordination between mechanical components and the on-board electronics. Fig.13 illustrates the normalized step response of the four joints and the grinder's motor, controlled by position controllers and a velocity controller, respectively. All responses are collected without any operational load, i.e., only inertial load presents. The rise time for Joint-1,-2, and -4 are less than $0.2s$. These joints are responsive because the inertial loads on these joints are inconsiderable compared to the joints' load capacities. Joint-3 experiences a slower response due to the speed-reduction gearbox and lead screw transmission. All actuators, including the grinder's motor, converge to the desired trajectory with zero steady-state error, proving the effectiveness of the implemented PID controllers.

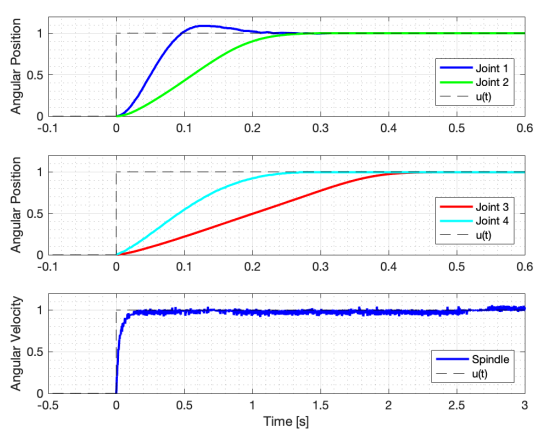

Fig. 13. Actuator responses of the four joints and the grinder's motor. The signals are normalized to a unit step. *Be aware with the different time-scales between subplots.*

B. Real-World Deployment

For the very first time, a real Contamination-Less In-Pipe Rehabilitation is conducted on a $100mm$-diameter corroded cast-iron pipe section. The anti-corrosion layer on the pipe section was removed and it was placed in a humid environment for six months. Tubercle asperities that are approximately 3-4mm tall developed on the pipe wall. Shown in Fig.14 is an illustration of the deployment setup. The CLR robot is attached to a fixture that simulates a grounded locomotion in-pipe robot. An external circulation device is grounded in adjacent to the L-IPR. It consists of two water pumps and a water storage. The circulation device is connected to the compartment of the mechanical seal. During the rehabilitation process, one pump fills the compartment with rinsing water, and the other pump retrieves the rinsing water into the storage, carrying the by-produced debris. A filter layer is integrated into the storage so that filtered water can be reused for circulation.

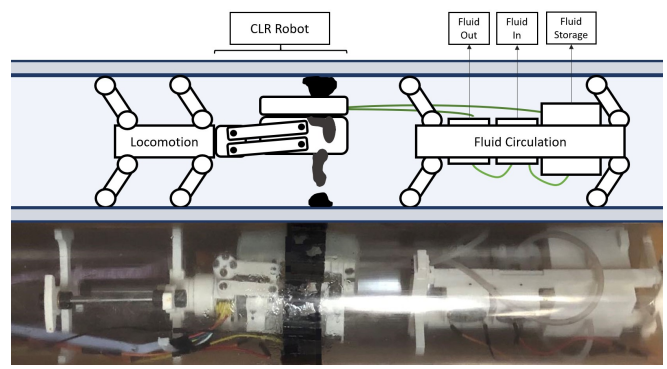

Fig. 14. Top: Schematics of the deployment setup. Bottom: Illustration of the deployment setup in a clear PVC pipe.

The manipulator engages the seal in Fig.15-A. The operator manually manipulates the grinder to remove the tubercle asperities. Since no visual feedback is available on-board, the operator postulates a sufficient removal when the grinding bit is in touch with the metal pipe wall, which can be easily suggested with a sudden increase in noise level. Fig.15-B demonstrates the result of the operation. An approximately $10mm$ by $15mm$ corroded area on the pipe surface is cleaned. The circulation device collects the by-produced debris and successfully circulates the rinsing water.

At the current stage, a controlled method to evaluate the quantitative effect of contamination containment is yet to be determined. In this work, the effectiveness is suggested in a few ways. First, there is no observable fluid leakage from the sealed enclosure during the operation. This can be further validated by the darkened color on the mechanical seal in Fig.15-C,-D, as it indicates a full contact between the seal and the pipe wall. Furthermore, in Fig.14-E, the residual debris on the filter layer of the water storage is displayed. The difference between -C and -D, as well as the filtered out debris, indicate an approximate amount of contamination that would have leaked into the pipeline.

Fig. 15. The CLR deployment in a real pipe. A: The seal creates a water-tight surface on the corroded pipe wall and the cleaning device operates inside. B: The cleaned surface. C: The seal after rinsing. D: The seal before rinsing (different operation from C). E: Filtered debris in the water storage.

VII. Discussion and Conclusion

In this study, a vital yet ignored aspect of rehabilitation in-pipe robots is identified. At present, no state-of-the-art R-IPR takes into consideration the by-produced contamination during the operation, which could lead to a detrimental effect on consumer health. Targeting this loophole, we propose the concept of 'Contamination-Less Rehabilitation', and the CLR robot, correspondingly. The CLR robot features three modules: a pipe-cleaning grinder, a compound mechanical seal, and an in-pipe manipulator. This work focuses on the manipulator, which features a novel nested-outer-inner manipulator configuration. We present the entire design and validation process in detail, such that the work can be heuristic to the general R-IPR community.

The CLR robot presents a novel manipulator layout that satisfies the CLR concept. More specifically, it is a layout that allows simultaneous operations of two end-effectors, with one's workspace fully enclosed by the other end-effector's physical volume. We believe this novel mechanism can extend to more than rehabilitation of water distribution pipes. A foreseeable application is on an explosive-diffusing robot. The CLR robot also provides a possible solution to miniaturization of R-IPRs, especially for deployment in sub-$100mm$ diameter pipes.

It is vital to realize room for improvements to the CLR robot. The real-world deployment result is rather qualitative. The future procedure involves setting up a more controlled environment to identify performance factors for robust design. On the other hand, the current position controller might easily lead to excessive deflection in the mechanical components when the operation is not conducted meticulously. One way to ameliorate this concern is with more advanced control laws such as an impedance controller. Another potential solution is to provide visual feedback to the operator, i.e., embedding vision in the manipulator.

The ultimate goal for this project is to deploy this robot to conduct a Contamination-Less Rehabilitation task in an in-service network. As a fully functional CLR robot is constructed, the next step is to optimize individual components, such as the SEA joint and the cleaning device. Ongoing research is to integrate linear serial elasticity in the pipe-cleaning device to provide force feedback element and further prevent hardware damage. From the workflow aspect, end-effectors for the leak repair and post-treatment tasks are to be developed before a comprehensive rehabilitation can be conducted.

References

[1] S. Folkman, "Water main break rates in the USA and Canada: A comprehensive study," pp. 1–49, 2018.
[2] European Environment Agency, "European waters - current status and future challenges: Synthesis," tech. rep., 2012.
[3] ASCE, "Water Infrastructure - ASCE's 2017 Infrastructure Report Card," tech. rep., American Society of Civil Engineers (ASCE), 2017.
[4] R. Morrison, J. Matthews, S. Sinha, and R. Sterling, "State of technology for rehabilitation of water distribution system," tech. rep., U.S. Environmental Protection Agency (EPA), 2013.
[5] N. Truong-Thinh, N. Ngoc-Phuong, and T. Phuoc-Tho, "A study of pipe-cleaning and inspection robot," *2011 IEEE International Conference on Robotics and Biomimetics, ROBIO 2011*, pp. 2593–2598, 2011.
[6] L. A. Mateos and M. Vincze, "In-pipe cleaning mechanical system for DeWaLoP - Developing water loss prevention," *Proceedings of the Austrian Robotics Workshop 2013*, pp. 1–6, 2013.
[7] PROKASRO, "KASRO Working Robot," 2018.
[8] E. Lambertini, S. K. Spencer, B. A. Kieke, F. J. Loge, and M. A. Borchardt, "Virus contamination from operation and maintenance events in small drinking water distribution systems," *Journal of Water and Health*, vol. 9, no. 4, pp. 799–812, 2011.
[9] A. Ercumen, J. S. Gruber, and J. M. Colford, "Water distribution system deficiencies and gastrointestinal illness: A systematic review and meta-analysis," *Environmental Health Perspectives*, vol. 122, no. 7, pp. 651–660, 2014.
[10] A. Selvakumar and A. N. Tafuri, "Rehabilitation of aging water infrastructure systems: Key challenges and issues," *Journal of Infrastructure Systems*, vol. 18, no. 3, pp. 202–209, 2012.
[11] Y. Yeung, E. Genevriere, and K. Youcef-Toumi, "Design of a mechanical sealing device for robotic water distribution pipe rehabilitation," *2020 International Mechanical Engineering Congress Exposition*, 2020 [Accepted].
[12] D. M. Chatzigeorgiou, K. Youcef-Toumi, A. E. Khalifa, and R. Ben-Mansour, "Analysis and design of an in-pipe system for water leak detection," pp. 1007–1016, 2012.
[13] Y. Wu, K. Kim, M. F. Henry, and K. Youcef-Toumi, "Design of a leak sensor for operating water pipe systems," *IEEE International Conference on Intelligent Robots and Systems*, vol. 2017, pp. 6075–6082, 2017.
[14] D. M. Chatzigeorgiou, A. E. Khalifa, K. Youcef-Toumi, and R. Ben-Mansour, "An in-pipe leak detection sensor: Sensing capabilities and evaluation," *ASME 2011 International Design Engineering Technical Conferences & the 2011 ASME/IEEE International Conference on Mechatronic and Embedded Systems and Applications*, 2011.
[15] KA-TE PMO AG, "KA-TE Shuttering System," 2018.
[16] H. Jeong, J. Park, Y. Cho, and J. Cheong, "Tendon-driven multi-DOFs mini manipulation system with micro camera," in *International Conference on Control, Automation and Systems*, vol. 3, pp. 1064–1067, 2011.
[17] X. Duan, Y. Yang, and B. Cheng, "Modeling and analysis of a 2-DOF spherical parallel manipulator," *Sensors (Switzerland)*, vol. 16, no. 9, 2016.
[18] G. A. Pratt and M. M. Williamson, "Series elastic actuators," in *IEEE International Conference on Intelligent Robots and Systems*, 1995.